Kovove Mater. 49 2011 427–436
DOI: 10.4149/km_2011_6_427

Structure and thermal expansion behaviour of Al/C composites reinforced with unidirectionally aligned continuous high modulus C fibres

N. Beronská[1*], K. Iždinský[1], P. Štefánik[1], S. Kúdela Jr.[1], F. Simančík[1], I. Vávra[2], Z. Križanová[2]

[1] *Institute of Materials and Machine Mechanics, Slovak Academy of Sciences, Račianska 75, 831 02 Bratislava, Slovak Republic*
[2] *Institute of Electrical Engineering, Slovak Academy of Sciences, Dúbravská cesta 9, 841 04 Bratislava, Slovak Republic*

Received 10 June 2011, received in revised form 26 August 2011, accepted 5 September 2011

Abstract

The interface and thermal expansion behaviour of aluminium matrix composite (Al-3Mg) unidirectionally reinforced with continuous high modulus and high thermal conductivity carbon fibres Thornel K1100 were studied. The composite was prepared by gas pressure infiltration and was subjected to thermal cycling from room temperature to 350 °C.

It appeared that the current fibre–matrix-technology option effectively eliminated the undesired fibre matrix reaction. The Al_4C_3 carbide formation had been suppressed to that extent that their appearance in the structure was quite rare. However, TEM observations confirmed an amorphous layer at the fibre–matrix interface.

The thermal expansion of the composite is closely related to the expansion of fibres exhibiting negative coefficient of linear thermal expansion throughout the whole temperature range. This indicates that the interfacial bonding is relatively strong even without any excessive fibre–matrix reaction.

K e y w o r d s: metal matrix composites (MMCs), Al/C interface, thermal expansion, CTE

1. Introduction

Continuous carbon fibre reinforced Al composites are mostly recognized as structural materials with unique mechanical properties, particularly specific strength and stiffness. For this purposes polyacrylonitrile (PAN) base high strength C fibres are mostly used. However, the development of pitch based high modulus (HM) C fibres exhibiting high thermal conductivity (TC) and low coefficient of linear thermal expansion (CTE) opened the door for Al/C composites also for thermal management applications.

Al/C when compared e.g. with Cu/C composites will undoubtedly suffer from the lower thermal conductivity of Al ($TC_{Al} = 0.59\ TC_{Cu}$) and higher coefficient of linear thermal expansion ($CTE_{Al} = 1.40\ CTE_{Cu}$). However, lower density (ρ) of Al ($\rho_{Al} = 0.30\ \rho_{Cu}$) makes them ideal candidates for applications where heat sinks with low density are required.

The preparation of Al/C composites is due to the fibre–matrix reaction leading to the formation of Al_4C_3 carbide quite challenging. The reaction improves on one hand the interfacial bonding strength; however, when too excessive it can drastically weaken mechanical properties of the composite [1–3]. Moreover, the hygroscopic carbide undergoes a severe degradation when exposed to ambient conditions [4].

It appears that the formation of Al_4C_3 is not only thermodynamic but also a kinetic problem [4]. Here the technology of composite preparation with its particular time-temperature sequence of operations plays the key role.

Previously the technology of gas pressure infiltration (GPI) was used for the preparation of copper matrix composites reinforced with high modulus and high thermal conductivity carbon fibres [5, 6]. Now we have adopted this technology for the preparation of aluminium matrix composites reinforced with the

*Corresponding author: tel.: +421 2 49268 228; fax: +421 2 49268 312; e-mail address: ummsnber@savba.sk

Table 1. Properties of K1100 carbon fibres

Tensile strength (GPa)	3.10
Tensile modulus (GPa)	965
Density ($kg\,m^{-3}$)	2200
Filament diameter (μm)	10
Thermal conductivity in longitudinal direction ($W\,m^{-1}\,K^{-1}$)	900–1000
Thermal conductivity in transversal direction ($W\,m^{-1}\,K^{-1}$)	2.4
Longitudinal CTE at 21 °C (K^{-1})	-1.5×10^{-6}
Transversal CTE at 21 °C (K^{-1})	12.0×10^{-6}

same K1100 carbon fibres. The aim of this paper is to present results obtained by structural studies and thermal expansion measurements of this particular composite.

2. Experimental material and procedure

High modulus and high thermal conductivity pitch based Thornel K1100 carbon fibres with 2000 filaments in one tow have been used as continuous reinforcement in an aluminium matrix alloyed with 3 wt.% of magnesium (Al-3Mg).

As-received fibres with properties presented in Table 1 were unidirectionally aligned and slightly pressed into a Mo mould forming thus a fibrous preform. These rod-like preforms with the dimensions $13 \times 13 \times 50\,mm^3$ had been inserted into a high pressure autoclave and preheated in a vacuum ~ 45 Pa. Once the infiltration temperature of 750 °C had been reached, fibre preform was immersed into a graphite crucible with a molten matrix metal and the system was allowed to thermally equilibrate for roughly 5 min. Subsequently argon gas pressure was applied up to 5.0 MPa within 2 min. Afterwards the composite was pulled out from the molten metal in order to let the matrix metal solidify and the sample cool outside the crucible.

Structural observations on as-received samples were performed with field emission scanning electron microscopy (SEM – JEOL 7600 FEG); chemical compositions were analysed using energy dispersive (EDS) X-ray spectroscopy (Oxford Instruments INCA microanalysis system with X-Max 50 detector). Structural studies were further performed with conventional transmission electron microscopy (TEM – JEOL 1200 EX). Ion milling at 5 kV accelerating voltage was applied for preparation of thin foils for TEM observations.

Composite samples with the dimensions of $4 \times 4 \times 10\,mm^3$ were used for linear thermal expansion measurements in both longitudinal (L) and transversal (T) directions. Designation L and T corresponds to fibre alignment direction with respect to longitudinal sample axes. Samples were subjected to three consequent heating and cooling cycles at the heating/cooling rate of $3\,K\,min^{-1}$ in an argon atmosphere using LINSEIS L75VS 1600C dilatometer equipped with a silica holder. Samples were cycled in the temperature range 30 °C to 350 °C. Each thermal cycle started with the sample preheating at 30 °C for 30 min, followed by heating and subsequent cooling back to the room temperature. One-hour rest time had been included before the next cycle started. Instantaneous CTE values were calculated from the strain––temperature curves as a function of temperature using LINSEIS TAWIN software. All CTEs were calculated in the temperature range 50 °C to 300 °C in order to eliminate the effect of non-steady state transient stages occurring at the beginning and at the end of heating and cooling periods.

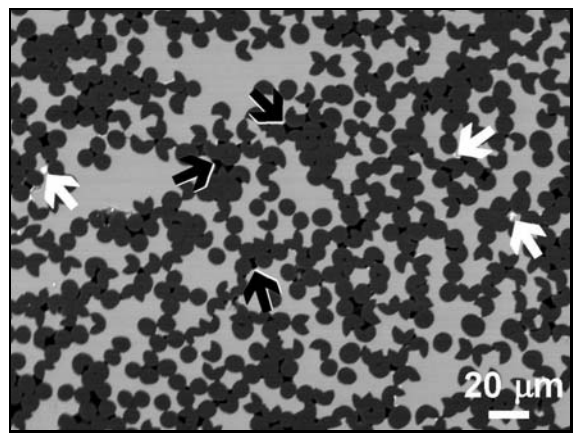

Fig. 1. Back-scattered electron micrograph of the cross sectional view of the structure of as-infiltrated Al-3Mg/K1100 composite.

3. Results

3.1. Structural studies

Structure of as-infiltrated Al/C composite is shown in Fig. 1. The composite exhibits relative homogeneous distribution of C fibres and fibre clusters. Some small black pores (marked with black arrows) ap-

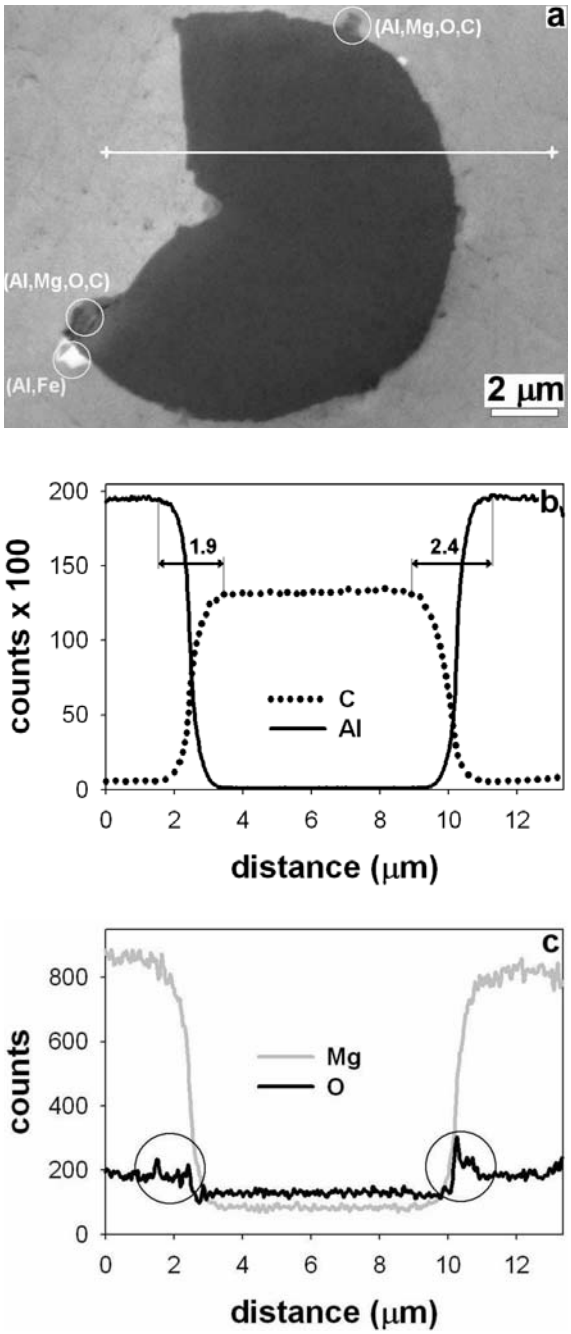

Fig. 2. Secondary electron micrograph of K1100 fibre in the Al-3Mg matrix (a), Al and C elemental linescans along the ++ acquisition line in Fig. 2a (b), Mg and O elemental linescans along the ++ acquisition line in Fig. 2a (c).

pearing mostly in the inter-fibre locations and white particles can be easily recognized. The average fibre volume content as determined via image analysis in 5 different locations was 57.6 %.

White particles marked with white arrows in Fig. 1 contain significant amounts of iron representing a typical impurity in aluminium alloys. Besides these, also some grey particles appear quite frequently at the

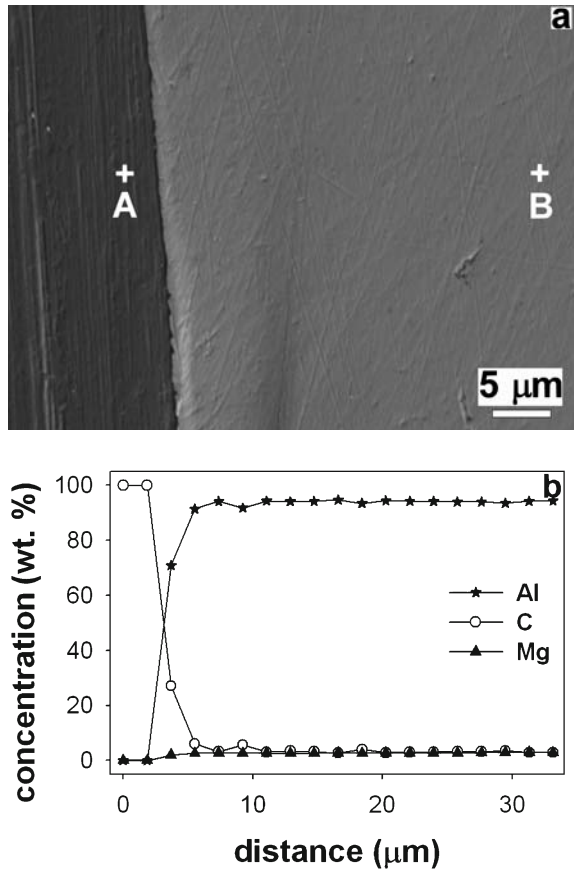

Fig. 3. Secondary electron micrograph of the fibre–matrix interface in the longitudinal section of Al-3Mg/K1100 composite (a), results of semiquantitative EDS analysis between points A and B in Fig. 3a (b).

fibre–matrix interface. EDS analysis confirmed that these particles contained different amounts of Al, Mg, C and O as shown in Fig. 2. The particles are quite small. The white circles indicate the X-ray generation region for Al. Due to actual densities this region is smaller for Fe and larger for Mg and C.

The fibre–matrix interface was characterized by elemental line scanning utilizing the X-ray signal of particular energy range for Al, C, Mg and O. Corresponding results are presented in Fig. 2b,c. It appeared that there was no continuous layer of any reaction product at the fibre matrix interface within the resolution of EDS. Only slight increase of oxygen marked with black circles in Fig. 2c can be recognized in the interfacial zone.

The distribution of elements close to fibre matrix interface was characterized also by EDS point analysis in 19 beam positions between A and B in Fig. 3. Neither these results presented in Fig. 3b confirmed any distinct interfacial reaction zone. The distribution of oxygen in longitudinal section of composite was finally analysed by element mapping as shown in Fig. 4a. Increased concentration of oxygen was preferentially found at the fibre–matrix interface.

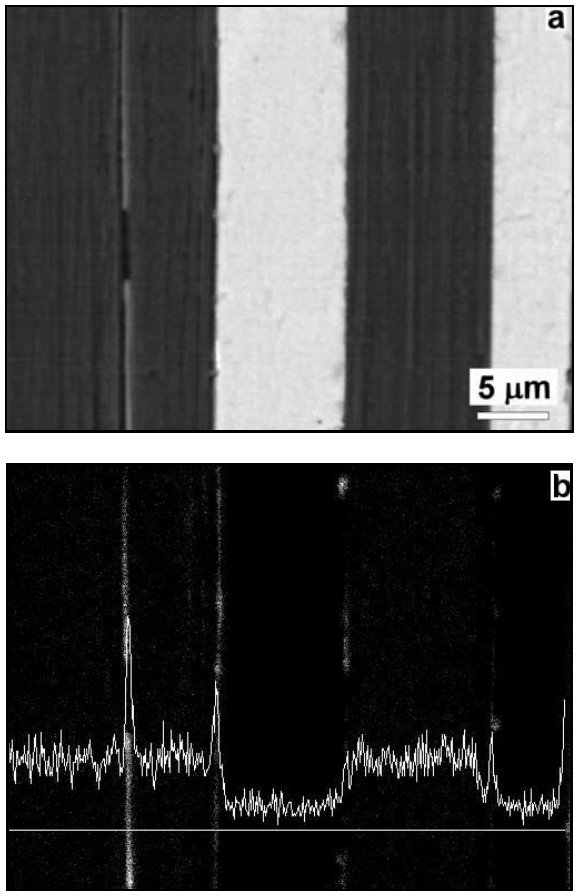

Fig. 4. Secondary electron micrograph of the structure of Al-3Mg/K1100 composite in longitudinal section (a), oxygen elemental linescan acquired along the white horizontal acquisition line superimposed on EDS element map revealing the distribution of oxygen in the structure shown in Fig. 4a (b).

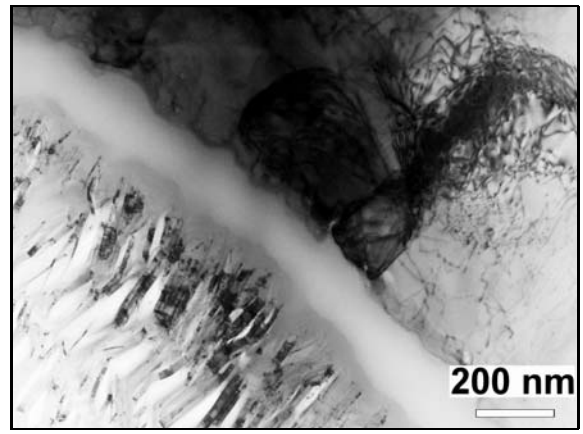

Fig. 5. Bright field TEM micrograph revealing stacked graphite layers inside the fibre and an amorphous interfacial layer in cross sectional view of the Al-3Mg/K1100 composite.

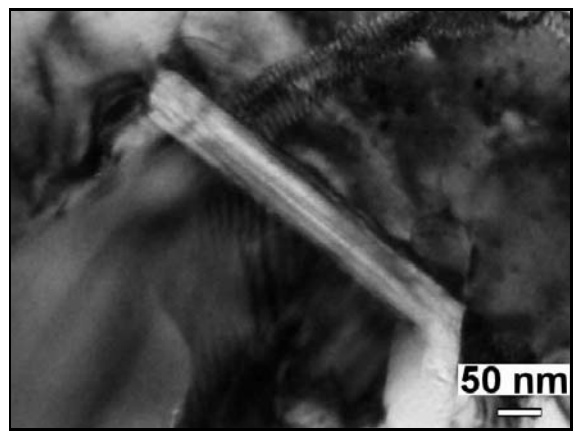

Fig. 6. Bright field TEM micrograph revealing Al_4C_3 crystal in the interfacial zone of Al-3Mg/K1100 composite.

TEM observations revealed an amorphous 100 to 400 nm thick layer at the interface. Typical example is shown in Fig. 5. The contrast inside the layer indicates that it may even be formed by two different layers. Selected area electron diffraction yielded only diffuse spectra from these layers. The determination of their chemical composition requires additional TEM analytical techniques.

Al_4C_3 carbide is known to exhibit needle-like morphology in Al/C composites [2, 7–10]. It should be stressed out that Al_4C_3 needles as presented in Fig. 6 were observed quite exceptionally in the current composite. This low frequency of appearance in the current composite confirmed that their formation had been effectively suppressed using the current set of conditions.

3.2. Thermal expansion

The temperature dependences of relative elongation and CTE of Al-3Mg/K1100 composite are presented in Figs. 7 and 8. The recorded curves reveal large differences in relative elongations in L and T directions.

As shown in Fig. 7a slight difference was recorded between the course of the first and the two rest thermal cycles in L direction whereas second and third cycles are nearly identical. The relative elongation increases to the temperature of about 67 °C and then decreases up to the end of the heating period. The length of the sample is shorter at 350 °C than at room temperature. All three cycles exhibit hysteresis – i.e. the heating and cooling values do not coincide, however, no actual permanent strains appeared at the end of applied thermal cycles.

Completely different course of temperature dependences of relative strain was recorded in T direction. Here the relative elongation monotonously increases with increasing temperature within the whole

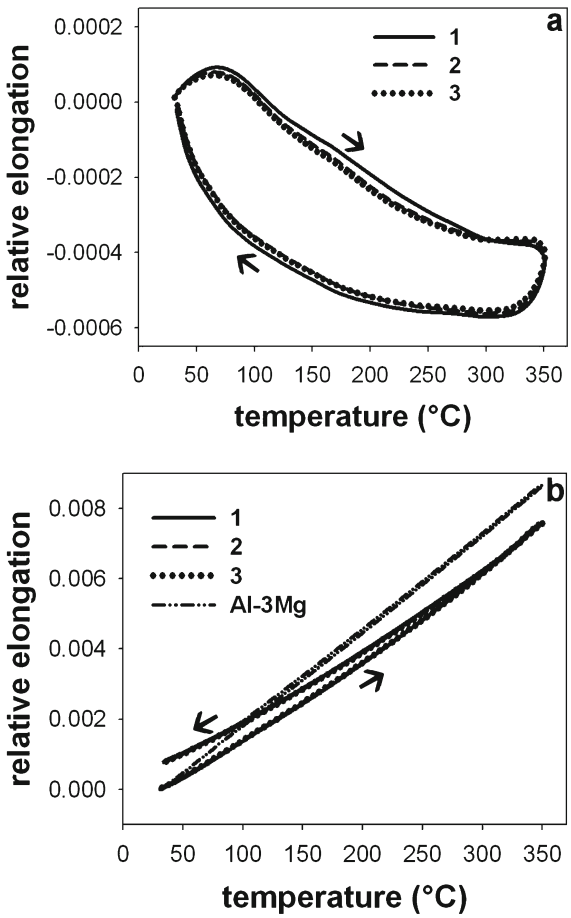

Fig. 7. Temperature dependences of relative elongation of Al-3Mg/K1100 composite subjected to three consecutive thermal cycles in L (a) and T directions compared with Al-3Mg matrix alloy (b).

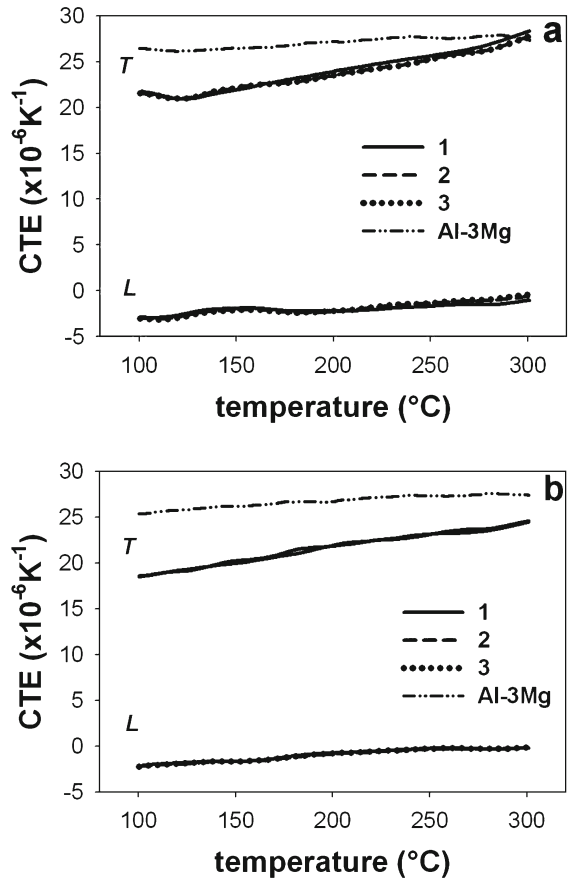

Fig. 8. Temperature dependences of CTE of Al reference and Al-3Mg/K1100 composite subjected to three consecutive thermal cycles during heating (a) and cooling periods (b).

Table 2. Mean coefficients of linear thermal expansion of Al-3Mg/K1100 composite in the temperature range 100 °C to 300 °C

	Heating	Cooling
CTE_L (10^{-6} K^{-1})	–1.9	–1.0
CTE_T (10^{-6} K^{-1})	23.8	21.6

heating period. The course of all three thermal cycles is identical exhibiting permanent elongations of about 7.8×10^{-4}.

CTEs in Fig. 8 further confirm the anisotropy of the composite. They point out slightly different character of the first thermal cycle in the L direction, and confirm the coincidence of all thermal cycles in T direction.

The temperature dependences of CTE in the second and third cycles exhibit certain linearity in the temperature range 100 to 300 °C. The mean coefficients of thermal expansion in this temperature range are presented in Table 2. Comparison of obtained CTEs shows that the expansion of composite in L direction is negative in both, i.e. heating and cooling periods, demonstrating thus the fundamental thermal expansion reduction due to fibres.

4. Discussion of results

4.1. Structural studies

A basic requirement for any satisfactory metal matrix composite is a good fibre–matrix bond [11]. The ideal case would be a matrix and a fibre which are mutually insoluble and non-reacting, where only wetting occurs between them with modest diffusion bonding [12]. This however is not the case of Al/C composites where no spontaneous wetting occurs between fibre and matrix [13–15]. This is accompanied by dissolution of fibres in the matrix and formation of un-

desirable and brittle Al_4C_3 carbide. Both these effects cause severe deterioration of the composite quality.

However, Al/C system can be modified by slight amounts of alloying additives, which change the solubility of the fibre atoms in a metal matrix. Calculations performed in [11, 12] revealed that the best additives to suppress the solubility of C in Al and thus the formation of Al_4C_3 carbide were silicon and magnesium. These were experimentally confirmed in [7] where Al matrix alloyed with different amounts of Mg was used to prepare Al/C composite via gas pressure infiltration. It was shown that increasing amount of Mg (0-8.5 wt.%) can even fully suppress the formation of brittle Al_4C_3 phase, resulting in an intermediate interfacial bonding with improved mechanical properties. Similar results were achieved with the additions of silicon [11, 12].

It is assumed [4] that the decreased tendency for carbide formation with increasing third element content is to be related to reduced carbon solubility in Al matrix and to the segregation of this element on the fibre–matrix boundary resulting in the increase of diffusion barrier for C diffusion hindering thus the diffusion-dependent Al_4C_3 formation. Mg was the prime choice for alloying of Al matrix in this work due to its higher TC and lower density when compared with Si.

Structural studies revealed that the fibre distribution in the sample volume is quite homogeneous. This is mostly due to the high fibre volume content that does not allow any large redistribution of fibres. This high volume content with densely packed fibres is one of the limitations of infiltration techniques when homogeneous distribution of fibres is required.

Closer inspection performed at higher magnification revealed that fibres anyway tend to group into clusters. The unidirectional alignment of continuous long fibres forms free channels in the inter-fibrous locations that enhance the molten metal penetration. However, the metal needs to enter the preform predominantly from the front (face) side. When it comes from the flank side it presses on fibres arranging them into clusters in different mould locations. In this case the fibre distribution is not completely homogeneous and the frequency of appearance of non-infiltrated locations increases.

The tendency towards incomplete metal penetration is further enhanced by poor wetting in the Al-C system. Wetting of graphite with aluminium and its alloys sharply improves only with temperature growth above 1150 ℃. According to data [16], aluminium at 1200 ℃ spreads on graphite up to wetting angle 38° after 13 min, then process stops and an intensive formation of aluminium carbides follows. These parameters required to improve wetting lie significantly above those used in this work.

If there is enough space for the molten metal to penetrate into the preform it can fill the empty spaces. The external gas pressure can keep it there until solidification. Finally, as shown in [5], the matrix metal remains trapped in the inter-fibrous locations even without any interfacial reaction. Pores appearing mostly in the fibre clusters might be due to insufficient metal penetration but also to matrix shrinkage on cooling.

SEM/EDS inspection revealed that various particles appear at the fibre matrix interface. Most frequently appearing are iron containing particles and oxide particles as shown in Fig. 2. The precise EDS quantitative analysis is difficult as the particles are smaller than the diameter of the excited volume, i.e. X-ray generation region for given acceleration voltage of 10 kV equals to 1.11 μm for Al, 1.72 μm for Mg, 1.32 μm for C and 0.38 μm for Fe. Therefore the acquired spectra represent rather the composition of particles with some contribution of adjacent matrix and fibre. The true phase identification based on the acquired EDS spectra is not possible.

The distribution of elements as revealed by elemental lines cans showed that within the resolution of EDS there was no reaction layer formed by Al and C at the fibre–matrix interface. The width of the zone where both elements appear corresponds to the diameter of the excited volume due to interaction of electron beam with the sample. The segregation of Mg atoms in the interfacial region was not observed as well. On the other hand, the increased concentration of oxygen atoms was quite clear.

The distribution of atoms as-revealed via elemental lines cans yields no sufficient quantitative information. Therefore the composition across the interface was further analysed via EDS point analysis making use of 100 s acquisition time. The aim was to confirm quantitatively whether there had been some increased concentration of Mg atoms in the interfacial region or not. It appeared that the concentration of Mg in the matrix is quite constant: 2.69 ± 0.12 wt.%. No increase in the concentration of Mg atoms was confirmed in the interfacial zone. The vast majority of Mg with respect to the binary Al-Mg equilibrium diagram is expected to be soluted in Al.

Element mapping finally confirmed selected concentration of oxygen atoms at the interface. Similar result was achieved with interfacial analysis preformed in [17], where a 0.3–0.4 μm thick spinel layer ($MgAl_2O_4$) was observed between the high modulus P100 graphite fibre and the 6061 Al matrix.

TEM analysis of the current composite however revealed that the fibre–matrix reaction resulted in the formation of interfacial amorphous layer. This is more in agreement with [8] where nanometric (5–10 nm) amorphous O-C-Al layer preferentially oriented along K1100 fibre – 2014 alloy was observed. The formation of both spinel [17] or O-C-Al amorphous layer

[8] is believed to be the result of chemical reaction between any absorbed oxygen at the fibre surface and the aluminium matrix at the interface during infiltration. Because the thickness of the amorphous layer is below 400 nm it could not be precisely analysed by EDS.

The formation of Al_4C_3 precipitates can hardly be completely avoided. It is well known that the formation of Al_4C_3 is thermodynamically favoured at temperatures below 2137 °C [18]. Moreover, since the C solubility in liquid Al is rather low (below 0.22 at.% at 800 °C) [19], it is thermodynamically difficult to prevent the precipitation of Al_4C_3 during or after melt infiltration [8]. Extremely low frequency of appearance confirms that its formation in the current composite is quite rare. Several factors may have contributed to this, although it is difficult to estimate to what extent each. The use of high modulus fibre with its graphite structure, the addition of Mg and the short time of exposure at the infiltration temperature can be outlined.

On the other hand the missing Al_4C_3 indicates rather weak interface. In the current composite the interfacial bonding is accomplished via amorphous reaction layer that can be even more beneficial to the composite than the non stable Al_4C_3 carbide. Moreover, it is known that in composites with weak interfaces, once a crack is nucleated in a brittle fibre, the possibility of interfacial debonding and sliding permits the broken fibre to pull-out, reducing thus the effect of stress concentration at the fibre break and avoiding catastrophic propagation of the crack [2].

4.2. Thermal expansion

Thermal expansion measurements relate directly measured expansion of sample with indirectly determined temperature. There had been an unambiguous discussion concerning the effect of apparatus on the thermal expansion recorded in recent years.

Kumar pointed out that thermocouple in the dilatometer was placed just above the sample but not touching the sample. Therefore when resistance furnace was switched on, the temperature recorded by the thermocouple increased according to the rate of heat supplied by the furnace. However, a sample takes some time to homogenize the temperature, and sample temperature is equal to thermocouple temperature only after some time when steady state is reached [20].

Hysteresis and residual strains in pure metals and unreinforced alloys have been reported earlier. Tjong et al. have attributed the hysteresis and residual strains in pure Al to the internal stresses arising from temperature difference from interior to surface of the sample [21]. The apparent hysteresis and residual strains observed even for pure Al and QE alloy were attributed to deviations from linearity at the beginning and end of rating cycles, i.e., their origin is to be related to the instrument and not to the intrinsic material behaviour [22].

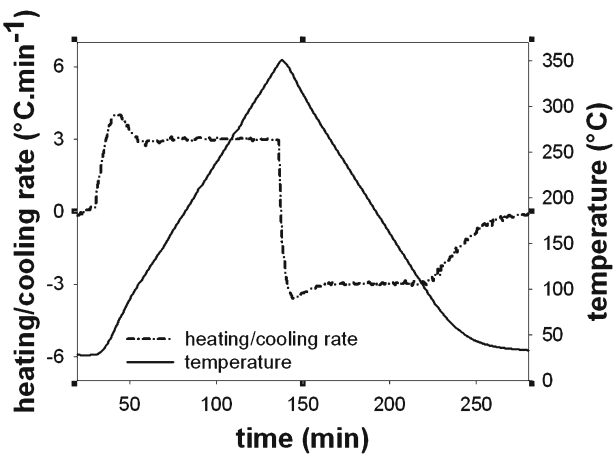

Fig. 9. Time dependences of heating/cooling rate and temperature within the thermal cycle.

On the other hand, Rudajevová [23] showed that the influence of the heating of support-tube and the push-rod on the measured results could be excluded by proper calibration of the dilatometer. The calibration function shows hysteresis. The temperature dependences of the relative elongation of pure metals or alloys show no hysteresis. Generally, the hysteresis can be observed even for alloys if the alloy is composed from two or more phases with the different thermal properties. This alloy behaves as a composite [23].

The time dependences of heating/cooling rate and temperature within one thermal cycle in the dilatometer used in this work are presented in Fig. 9. As can be seen there are some deviations from the heating/cooling rate of $3\,\mathrm{K\,min^{-1}}$ particularly at the beginning of the heating period: after the switch from heating to cooling and at the end of cooling period. These were recorded by the thermocouple indicating predominantly the temperature of the furnace close to the sample surface. The actual temperature inside the sample is further modified by thermal conductivity of the composite. For the sake of measurement interpretation it is supposed to be identical with that of the thermocouple.

However, composites with unidirectional alignment of reinforcing fibres exhibit large anisotropy of properties. In some sense they might be regarded more in terms of structural parts than in terms of a material. The particular distribution of reinforcing fibres is decisive not only for mechanical properties but also for the thermal conductivity of the composite. Large differences in TC for the current Al-3Mg/K1100 composite were confirmed already in [24]. The TC in L direction was $540.8\,\mathrm{W\,m^{-1}\,K^{-1}}$ whereas in T direction only $25.4\,\mathrm{W\,m^{-1}\,K^{-1}}$. All this indicates that the

results of thermal expansion measurements should be interpreted with caution.

Comparison of the thermal expansion data reveals slightly different course of the temperature dependences of the relative elongation in the first thermal cycle, very similar relative elongations in the second and third cycles and distinct knees appearing nearly at the same temperatures for all three cycles in the L direction. No permanent strains, i.e., neither length contractions nor elongations were recorded.

The course of relative strain in the first cycle is influenced by the as-received condition of the composite reflecting the thermal and mechanical history associated with the manufacturing process. Here the cooling from the infiltration temperature of 750 °C is the source of residual thermal stresses occurring in composite due to different thermal and mechanical properties of fibres and matrix. There are no thermal stresses within the composite at the matrix melting point. As the composite cools, the metal matrix contracts to a significantly larger extent than the fibre reinforcement. The thermal stresses are temperature dependent and they influence the dilatational characteristics of the composites [25]. However, residual strains appearing as a consequence of manufacturing process are mostly released during the first heating as revealed in related papers [26–29] and confirmed also in this work. It is obvious that residual strains increase with increasing manufacturing temperature, as shown for Cu/K1100 composites in [5]. The slight difference between the first and subsequent two cycles is due to low manufacturing thermal stresses in as received composite due to cooling from relatively low infiltration temperature of 750 °C when compared e.g. with 1200 °C for copper matrix [5].

Particular cycles exhibit a distinct knee in the heating segment on the temperature dependence of relative elongation in L direction in all three cycles. Relative elongations do rapidly increase in the temperature range 30 °C to 67.6 °C (1st cycle), 65.1 °C (2nd cycle) and 64.3 °C (3rd cycle), and then decrease up to 350 °C. In the temperature range from 300 to 350 °C a typical non-steady state transient stage occurs [20]. This is to be related to conversion of heating to cooling mode. In the course of cooling, monotonous relative elongation decrease takes place in the temperature range 350 °C down to 30 °C.

This behaviour can be qualitatively explained taking into account the shear stress of the matrix and thermal expansion of fibres. Due to differences in CTE of matrix and fibres, matrix is in residual tension and fibres in residual compression after manufacturing cooling (as-received condition). As the CTE of matrix is $23.1 \times 10^{-6}\,K^{-1}$ and that of fibres even negative $-1.5 \times 10^{-6}\,K^{-1}$, the matrix residual tension is relatively quickly relieved during heating. Compressive stress in the matrix builds up with progressive heating. As soon as the compression yield stress is reached the operation of creep mechanism begins stress relief. The knee is coincidental with the start of this stress relief leading to the decrease of relative elongation as analysed by Dutta [17]. In the case of strong interface this tendency proceeds up to the highest temperature. At the end of the heating half-cycle (at 350 °C), only a small axial compressive stress is left in the matrix. During cooling, the compressive stress is quickly relieved, and a tensile stress builds up throughout the rest of the temperature excursion [17].

The relative elongations of composite in T direction exhibit permanent strain (elongation) in all three cycles. This can be explained by the constant volume of the matrix during yielding [30]. As the temperature rises, the matrix is primarily stressed in compression along the fibre axis and it starts to yield at some point. Nevertheless, the matrix flow along the fibre axis is limited when the fibre/matrix bond is strong enough. At the same time, the matrix yielding transversely to the fibre axis is only little restricted enabling thus large transversal plastic strain [31].

Permanent elongation in all three cycles is to be related to lower pore content in the current Al-3Mg/K1100 composite. As shown in [5] the less perfect infiltration of Cu-K1100 composite with larger pores provides more space for the matrix to expand within the sample. Therefore, the permanent strain of this composite is smaller than that of CuCr1-K1100 where the stronger interfacial bonding is supposed.

On the other hand, permanent strain in current composite in T direction can be explained only if forming of new pores is admitted. The extent of this strain is expected to decrease in further thermal cycles due to the fact that the matrix will get the opportunity to expand into pores diminishing thus the increase of the sample volume.

The temperature dependence of CTE for K1100 fibres is not known. However, the analysis performed with similar pitch based high modulus carbon fibres P100 using the measurement of diffracted intensity of an argon laser [32] indicates that the contraction of fibres continuously proceeds up to the temperature of about 450 °C.

The expansion of current composite in L direction is governed primarily by the expansion of K1100 fibres as confirmed by the negative CTE_L for both heating and cooling segments. This is possible only due to the fact that the interfacial bonding is strong enough to restrict the expansion of matrix. The CTE_L ($-1.9 \times 10^{-6}\,K^{-1}$ for heating and $-1.0 \times 10^{-6}\,K^{-1}$ for cooling) is even slightly lower when compared with those recorded for Cu/K1100 ($-0.6 \times 10^{-6}\,K^{-1}$ for heating and $0.1 \times 10^{-6}\,K^{-1}$ for cooling) and Cu-1Cr/K1100 ($0.1 \times 10^{-6}\,K^{-1}$ for heating and $-0.1 \times 10^{-6}\,K^{-1}$ for cooling) composites in the equal temperature range 100–300 °C [24].

In this sense the interfacial bonding in Al-3Mg/K1100 composite, although without any intense Al-C interfacial reaction leading to the formation of Al_4C_3 carbide, is strong enough to keep the structural stability of material in the temperature range up to 350 °C.

5. Conclusions

Structural studies and thermal expansion measurements of Al-3Mg/K1100 unidirectionally reinforced composite were performed in this work.

It appeared that the current choice of fibre–matrix-technology selection effectively eliminated the undesired fibre matrix reaction.

The Al_4C_3 carbide formation had been suppressed to that extent that their appearance in the structure was quite rare.

EDS analysis performed on bulk samples did not reveal any reaction layer at the interface but increased concentration of oxygen in the interfacial region.

TEM observations revealed an amorphous layer most probably formed by chemical reaction between any absorbed oxygen at the fibre surface and the aluminium matrix at the interface during infiltration.

The thermal expansion measurements confirmed the large anisotropy of properties in L and T directions.

The thermal expansion in L direction is distinguished by a maximum at about 65 °C. This is related to the start of the stress relief after the compression yield stress of the matrix had been reached.

The thermal expansion in T direction exhibited some permanent elongation resulting from the plastic deformation of the matrix within the thermal cycle.

The thermal expansion of the composite is closely related to the expansion of fibres exhibiting negative CTE throughout the whole temperature range.

This indicates that the interfacial bonding is strong enough even without any excessive fibre–matrix reaction.

Acknowledgements

This work has been accomplished within the project "Building of the Centre of excellence for research and development of structural composite materials – 2nd stage" (ITMS: 26240120020) supported by the Operational Programme Research and Development using the financial assistance from the European Regional Development Fund (ERDF). The contribution of the infrastructure of research and development acquired within the project "Establishment of the Centre of excellence for research and development of structural composite materials for machine, construction and medical applications" is highly acknowledged (ITMS: 26240120006). There are also highly acknowledged the Grant Agency VEGA (Project 2/015/10) and the Slovak Agency for Science and Research (Project VMSP-P-0036-07).

References

[1] LI, S. H.—CHAO, C. G.: Metall. Mater. Trans. A-Phys. Metall. Mater. Sci., *35A*, 2004, p. 2153. http://dx.doi.org/10.1007/s11661-004-0163-z
[2] VIDAL-SETIF, M. H.—LANCIC, M.—MARHIC, C.—VALLE, R.—RAVIART, J. L.—DAUX, J. C.—RABINOVITCH, M.: Mater. Sci. Eng. A: Struct. Mater. Prop. Microstruct. Process., *272*, 1999, p. 321.
[3] YANG, M.—SCOTT, V. D.: J. Mater. Sci., *26*, 1991, p. 1609. http://dx.doi.org/10.1007/BF00544671
[4] ETTER, T.—SCHULZ, P.—WEBER, M.—METZ, J.—WIMMLER, M.—LOFFLER, J. F.—UGGOWITZER, P. J.: Mater. Sci. Eng. A, *448*, 2007, p. 1. http://dx.doi.org/10.1016/j.msea.2006.11.088
[5] BERONSKÁ, N.—IŽDINSKÝ, K.—ŠTEFÁNIK, P.—SIMANČÍK, F.—ZEMÁNKOVÁ, M.— DVORÁK, T.: Kovove Mater., *47*, 2009, p. 175.
[6] IŽDINSKÝ, K.—SIMANČÍK, F.—KORÁB, J.—KRAMER, I.—ŠTEFÁNIK, P.—KAVECKÝ, Š.—ŠRAMKOVÁ, T.—CSUBA, A.—ZEMÁNKOVÁ, M.: Kovove Mater., *44*, 2006, p. 327.
[7] WANG, X.—JIANG, D.—WU, G.—LI, B.—LI, P.: Mater. Sci. Eng. A, *497*, 2008, p. 31. http://dx.doi.org/10.1016/j.msea.2008.07.022
[8] SEONG, H. G.—LOPEZ, H. F.—ROBERTSON, D. P.—ROHATGI, P. K.: Mater. Sci. Eng. A, *487*, 2008, p. 201. http://dx.doi.org/10.1016/j.msea.2007.10.081
[9] ZHANG, Y. H.—WU, G. H.: Trans. Nonferrous Met. Soc. China, *20*, 2010, 2148. http://dx.doi.org/10.1016/S1003-6326(09)60433-7
[10] LANCIN, M.—MARHIC, C.: J. Europ. Cer. Society, *20*, 2000, 1493. http://dx.doi.org/10.1016/S0955-2219(00)00021-2
[11] PELLEG, J.—ASHKENAZI, D.—GANOR, M.: Mater. Sci. Eng. A, *281*, 2000, p. 239. http://dx.doi.org/10.1016/S0921-5093(99)00718-2
[12] REVZIN, B.—FUKS, D.—PELLEG, J.: Compos. Sci. Technol., *56*, 1996, p. 3. http://dx.doi.org/10.1016/0266-3538(95)00123-9
[13] NAYEB-HASHEMI, H.—SEYYIDI, J.: Metal. Trans., *20A*, 1989, p. 727.
[14] KHAN, I. H.: Metall. Trans., *7A*, 1976, p. 1281.
[15] OH, S. Y.—CORNIE, J. A.—RUSSEL, K. C.: Metall. Trans., *20A*, 1989, p. 527.
[16] FEDOROV, V. B.—SHORSHOROV, M. H.—KHAKIMOV, D. K.: Carbon and its interaction with metals. Moscow, Metallurgy 1978.
[17] DUTTA, I.: Acta Mater., *48*, 2000, p. 1055.
[18] OKAMOTO, H.: J. Phase Equilib., *13*, 1992, p. 97. http://dx.doi.org/10.1007/BF02645389
[19] QIU, C.—METSELAAR, R.: J. Alloys Compd., *216*, 1994, p. 55. http://dx.doi.org/10.1016/0925-8388(94)91042-1
[20] KUMAR, S.—INGOLE, S.—DIERINGA, H.—KAINER, K. U.: Comp. Sci. Tech., *63*, 2003, p. 1805.
[21] TJONG, S. C.—TAM, K. F.—WU, S. Q.: Comp. Sci. Tech., *63*, 2003, p. 89. http://dx.doi.org/10.1016/S0266-3538(02)00200-2

[22] KUMAR, S.—MONDAL, A. K.—DIERINGA, H.—KAINER, K. U.: Comp. Sci. Tech., *64*, 2004, p. 1179. http://dx.doi.org/10.1016/j.compscitech.2003.09.022
[23] RUDAJEVOVÁ, A.—PADALKA, O.: Comp. Sci. Tech., *65*, 2005, p. 989. http://dx.doi.org/10.1016/j.compscitech.2004.11.001
[24] BERONSKÁ, N.: Metal Matrix Composites Reinforced with High Modulus Carbon Fibres Characterized by High Thermal Conductivity. [Doctoral Thesis]. Bratislava, IMMM SAS 2009.
[25] RUDAJEVOVÁ, A.—LUKÁČ, P.: Acta Mater., *51*, 2003, p. 5579. http://dx.doi.org/10.1016/S1359-6454(03)00421-X
[26] LUO, X.—YANG, Y.—LIU, C.—XU, T.—YUAN, M.—HUANG, B.: Scripta Mater., *58*, 2008, p. 401.
[27] RUDAJEVOVÁ, A.—MUSIL, O.: Kovove Mater., *43*, 2005, p. 210.
[28] RUDAJEVOVÁ, A.—LUKÁČ, P.: Kovove Mater., *46*, 2008, p. 145.
[29] LUKÁČ, P.—RUDAJEVOVÁ, A.: Kovove Mater., *41*, 2003, p. 281.
[30] NASSINI, H. E.—MORENO, M.—GONZALES, O. C.: J. Mater. Sci., *36*, 2001, p. 2759. http://dx.doi.org/10.1023/A:1017973132276
[31] KÚDELA, S. Jr.—RUDAJEVOVÁ, A.—KÚDELA, S.: Mater. Sci. Eng. A, *462*, 2007, p. 239. http://dx.doi.org/10.1016/j.msea.2006.05.173
[32] PRADERE, C.—SAUDER, C.: Carbon, *46*, 2008, p. 1874. http://dx.doi.org/10.1016/j.carbon.2008.07.035